Chapter 3

Physicochemical characterization of degradable thermosensitive polymeric micelles

Osamu Soga[1], Cornelus F. van Nostrum[1], Aissa Ramzi[1], Tom Visser[2], Fouad Soulimani[2], Peter M. Frederik[3], Paul H. H. Bomans[3] and Wim E. Hennink[1]

[1] Department of Pharmaceutics, Utrecht Institute for Pharmaceutical Sciences (UIPS), Faculty of Pharmaceutical Sciences, Utrecht University, Utrecht, The Netherlands
[2] Department of Vibrational Spectroscopy, Faculty of Chemistry, Utrecht University, Utrecht, The Netherlands
[3] EM-unit, Department of Pathology, Medical Faculty, University Maastricht, Maastricht, The Netherlands

Langmuir 20 (2004) 9388-9395

Abstract

Amphiphilic AB block copolymers consisting of thermosensitive poly(*N*-(2-hydroxypropyl) methacrylamide lactate) and poly(ethylene glycol), pHPMAmDL-*b*-PEG, were synthesized via a macroinitiatoir route. Dynamic light scattering measurements showed that these block copolymers form polymeric micelles in water with a size of around 50 nm by heating of an aqueous polymer solution from below to above the critical micelle temperature (CMT). The critical micelle concentration (CMC) as well as the CMT decreased with increasing pHPMAmDL block lengths, which can be attributed to the greater hydrophobicity of the thermosensitive block with increasing molecular weight. Cryo-transmission electron microscopy (cryo-TEM) analysis revealed that the micelles have a spherical shape with a narrow size distribution. ^{1}H NMR measurements in D_2O showed that the intensity of the peaks of the protons from pHPMAmDL block significantly decreased above the CMT, indicating that the thermosensitive blocks indeed form the solid-like core of the micelles. Static light scattering measurements demonstrated that pHPMAmDL-*b*-PEG micelles with relatively large pHPMAmDL blocks possess a highly packed core that is stabilized by a dense layer of swollen PEG chains. FT-IR analysis indicated that dehydration of amide bonds in the pHPMAmDL block occurs when the polymer dissolved in water is heated from below to above its CMT. The micelles were stable when an aqueous solution of micelles was incubated at 37 °C and at pH 5.0, where the hydrolysis rate of lactate side groups is minimized. On the other hand, at pH 9.0, where hydrolysis of the lactic acid side groups occurs, the micelles started to swell after 1.5 hours of incubation and complete dissolution of micelles was observed after 4 hours as a result of hydrophilization of the thermosensitive block. Fluorescence spectroscopy measurements with pyrene loaded in the hydrophobic core of the micelles showed that when these micelles were incubated at pH 8.6 and at 37 °C the microenvironment of pyrene became increasingly hydrated in time during this swelling phase. The results demonstrate the potential applicability of pHPMAmDL-*b*-PEG block copolymer micelles for the controlled delivery of hydrophobic drugs.

1. Introduction

Amphiphilic block copolymers consisting of a hydrophilic and a hydrophobic segment self-assemble into polymeric micelles in aqueous solution with a hydrophobic core stabilized by a hydrophilic shell [1,2]. Currently, polymeric micelles are extensively investigated for pharmaceutical applications [3-6] because of their attractive features as drug delivery vehicles. Hydrophobic drugs can be loaded into their hydrophobic core [7]. Moreover, the size of polymeric micelles is generally between 10 to 60 nm, which is relatively small compared to other colloidal drug carriers such as liposomes and emulsions. Due to their small size and hydrophilic surface, polymeric micelles are not easily recognized and captured by macrophages of the mononuclear phagocyte system (MPS). Therefore, polymeric micelles have a relatively long circulation time after intravenous administration, and as a result they accumulate in e.g. tumor and other inflammation tissues due to the so-called EPR (enhanced permeation and retention) effect [8]. Furthermore, the critical micelle concentration (CMC) of polymeric micelles is usually much lower than that of low molecular weight surfactant micelles, which ensures a good physical stability against dilution after injection into the bloodstream. Poly(ethylene glycol) (PEG) is most commonly used as the hydrophilic segment of the copolymers forming the micelles as well as for the coating of other colloidal drug carriers, because of its non-toxicity and good "stealth" properties [9,10]. On the other hand, a variety of polymers have been used as hydrophobic segment in polymeric micelles: poly(propylene glycol) (Pluronics®) [11], poly(aspartic acid) with chemically conjugated doxorubicin [12], poly(β-benzyl-L-aspartate) [7], and poly(ester)s such as poly(lactic acid) [13] and poly(ε-caprolactone) [14].

Recently, stimuli-sensitive polymers have been used in block copolymers for the preparation of intelligent drug carriers [15,16]. In particular, thermosensitive polymers, e.g. poly(*N*-isopropylacrylamide) (PNIPAAm) with its cloud point (around 32 °C in water) close to body temperature, have been investigated [17-19]. Block copolymers consisting of a thermosensitive PNIPAAm block and PEG indeed form micelles at 37 °C [20,21]. Destabilization of these micelles can be triggered by hypothermia or by the introduction of comonomers with hydrolyzable side groups [22,23].

Interestingly, it was reported in Chapter 2 that poly(*N*-(2-hydroxypropyl) methacrylamide lactate) (poly(HPMAm-lactate)) shows lower critical solution temperature (LCST) behavior in aqueous solution [24]. It is expected that due to hydrolysis of the lactic acid side groups the cloud point (CP) will increase in time with lactic acid, an endogenous compound, and pHPMAm as degradation products. pHPMAm is a water-soluble polymer and has shown to be non-toxic in clinical trials [25,26]. It was demonstrated that the CP of poly(HPMAm-lactate) can be well controlled by the length of the lactate acid side group (e.g.

monolactate or dilactate) and copolymer composition [24]. Among these polymers, in particular poly(HPMAm-dilactate) is an interesting polymer, because its CP (around 10 °C) is far below body temperature. It is expected that block copolymers of poly(HPMAm-dilactate) and PEG form polymeric micelles at 37 °C but gradually dissolve due to hydrolysis of the lactic acid side groups, by which a drug that is loaded in the hydrophobic core is released into the environment (Figure 1).

In this chapter, a number of block copolymers of poly(HPMAm-dilactate) and PEG (pHPMAmDL-*b*-PEG) were synthesized and the characteristics of polymeric micelles based on these block copolymers were investigated with cryo-transmission electron microscopy and light scattering techniques. The mechanism of the LCST behavior of poly(HPMAm-dilactate) was investigated with FT-IR and ^{1}H NMR spectroscopy. Finally, the destabilization behavior of the micelles was studied.

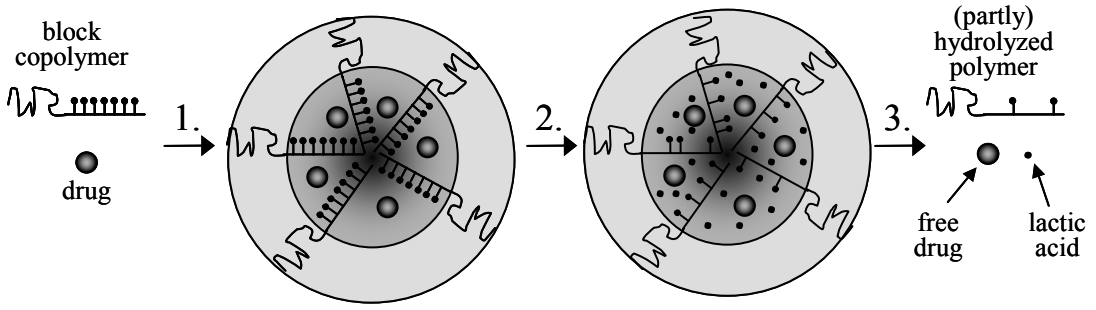

Figure 1. A schematic representation of the concept of polymeric micelles with controlled instability, formed from block copolymers with hydrolytically sensitive side groups. The numbered consecutive steps are the following: 1. Self-assembly and drug loading of polymeric micelles in water above the CMT. 2. Degradation and hydrophilization of the core. 3. Dissolution of the micelles and release of the drug.

2. Materials and methods

2.1. Materials

HPMAm esterified with optically pure di-*S*-lactic acid (further abbreviated as HPMAm-dilactate) was synthesized as described previously [23]. Monomethyl ether of poly(ethylene glycol) (mPEG), MW = 5,000 g/mol, was supplied by NEKTAR (San Carlos, CA, USA). 4,4-azobis(4-cyanopentanoic acid) (ABCPA) and pyrene were from Fluka, Chemie AG (Buchs, Switzerland). The PEG_2-ABCPA macroinitiator with PEG 5000 was prepared as described previously [22].

2.2. Synthesis of p(HPMAm-dilactate)-b-PEG block copolymers (pHPMAmDL-b-PEG)

pHPMAmDL-*b*-PEG block copolymers were synthesized by radical polymerization using HPMAm-dilactate as monomer and PEG_2-ABCPA as initiator. HPMAm-dilactate and PEG_2-ABCPA were dissolved at a total concentration of 0.3 g/mL in acetonitrile. To obtain block copolymers with different pHPMAmDL block lengths, the ratio of monomer to macroinitiator was varied between 35/1 to 140/1 (mol/mol). The polymerization was conducted at 70 °C for 24 hours in a nitrogen atmosphere. The polymers were collected by centrifugation after precipitation in diethyl ether. The polymers were purified by dissolving them in cold water, followed by filtration through a 0.22 μm filter and freeze-drying. The products were characterized by ^{1}H NMR with a Gemini 300 MHz spectrometer (Varian Associates Inc. NMR Instruments, Palo Alto, CA) and gel permeation chromatography (GPC). GPC was done using Plgel 3 μm MIXED-D + Plgel 3 μm MIXED-E columns (Polymer Laboratories) and poly(ethylene glycol) standards. The eluent was DMF containing 10 mM LiCl, the elution rate was 0.7 mL/min, and the temperature was 40 °C.

^{1}H NMR (solvent: $CDCl_3$) (see Scheme 1, all protons are from pHPMAmDL block except for methylene protons from PEG.): δ = 6.5 (b, CO-N<u>H</u>-CH_2), 5.0 (b, NH-CH_2-C<u>H</u>(CH_3)-O and CO-C<u>H</u>(CH_3)-O), 4.4 (b, CO-C<u>H</u>(CH_3)-OH), 3.6 (b, PEG methylene protons, O-C<u>H_2</u>-C<u>H_2</u>), 3.4 (b, NH-C<u>H_2</u>-CH(CH_3)), 2.0-0.6 (the rest of the protons from the pHPMAmDL block).

The number average molecular weight (M_n) of pHPMAmDL block was determined by ^{1}H NMR as follows: a) the value of the integral of the PEG protons divided by 454 (average number of protons per one PEG 5000 chain) gave the integral value for one PEG proton, and b) the number of HPMAmDL units in the polymers was determined from the ratio of the integral of the methine proton (CO-C<u>H</u>(CH_3)-OH) of HPMAmDL to the integral of one PEG proton. The number average molecular weight of the pHPMAmDL block was calculated from the resulting number of units.

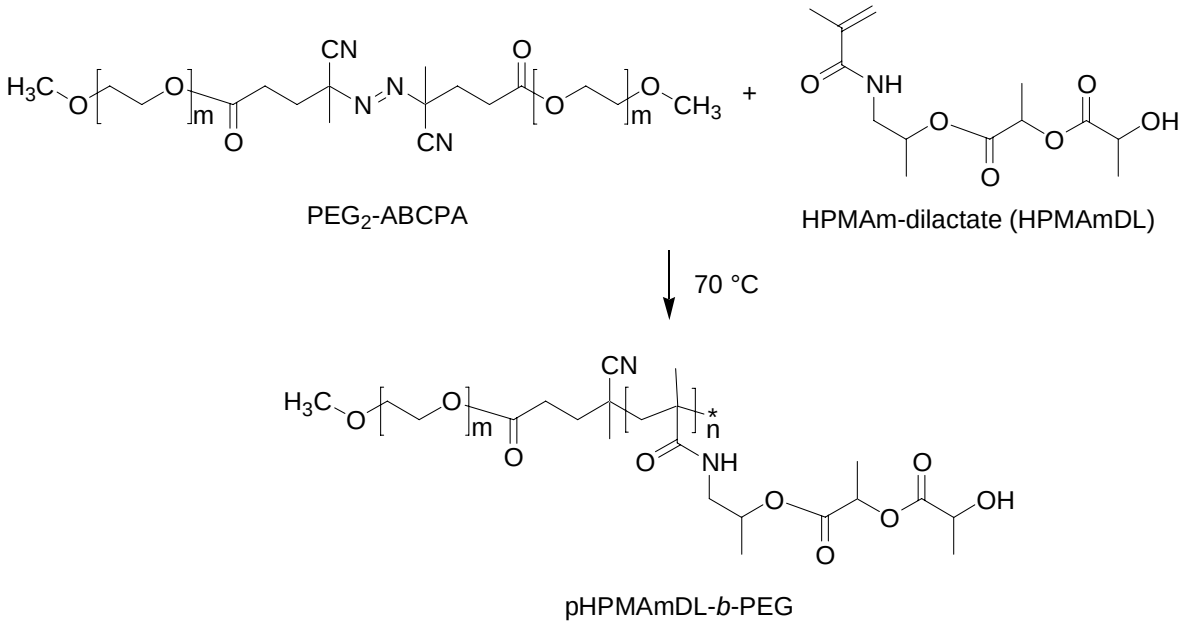

Scheme 1. Synthesis route and structure of pHPMAmDL-*b*-PEG block copolymers.

2.3. Determination of the critical micelle temperature (CMT)

The CMT of the different block copolymers was determined with static light scattering using a Horiba Fluorolog fluorometer (650 nm, at a 90° angle). The polymers were dissolved at a concentration of 10 mg/mL in isotonic 120 mM ammonium acetate buffer (pH = 5.0) at 0 °C. The scattering intensity was measured every 0.2 °C during heating and cooling (the heating/cooling rate was approximately 1 °C/min). Onsets on the X-axis, obtained by extrapolation of the intensity-temperature curves during heating to intensity zero, were considered as the CMT. The CMT determinations were done at least two times and the deviations were smaller than 0.5 °C.

2.4. Formation of micelles

Micelles of the different block copolymers were formed by a quick heating of an aqueous polymer solution from below to above the CMT [27]. The polymers were dissolved at a concentration between 0.1 to 20 mg/mL in isotonic 120 mM ammonium acetate buffer (pH = 5.0) at 0 °C. Then the polymer solution (1 mL) was quickly heated from 0 °C to 50 °C and left at 50 °C for 1 minute. For DLS and other measurements, the micelle solution was incubated at 37 °C or at room temperature.

2.5. Dynamic light scattering (DLS)

DLS measurements were done to determine the size of the micelles, using a Malvern 4700 system (Malvern Ltd., Malvern, UK) consisting of an Autosizer 4700 spectrometer, a pump/filter unit, a Model 2013 air-cooler argon ion laser (75 mW, 488 nm, equipped with a model 2500 remote interface controller, Uniphase) and a computer with DLS software (PCS, version 3.15, Malvern). The measurement temperature was 37 °C and the measurement angle was 90°. The change in solvent viscosity with temperature was corrected by the software.

2.6. Determination of the critical micelle concentration (CMC)

The CMC of the block copolymers was determined using pyrene as a fluorescencent probe [28]. Micelles of the different block copolymers were formed as described above in isotonic 120 mM ammonium acetate buffer (pH = 5.0) at a concentration of 2 mg/mL. The micellar solutions were cooled to room temperature and subsequently diluted with the same buffer yielding different polymer concentrations ranging from 1×10^{-5} to 1 mg/mL. Next, 15 μL of pyrene dissolved in acetone (concentration, 1.8×10^{-4} M) was added to 4.5 mL of polymer solution. The polymer solutions with pyrene were incubated for 20 hours at room temperature in the dark to allow evaporation of acetone. Fluorescence excitation spectra of pyrene were obtained as a function of the polymer concentration using a Horiba Fluorolog fluorometer (at a 90° angle). The excitation spectra were recorded at 37 °C from 300 to 360 nm with the emission wavelength at 390 nm. The excitation and emission band slits were 4 nm and 2 nm, respectively. The intensity ratio of I_{338}/I_{333} was plotted against polymer concentration to determine the CMC.

2.7. Static light scattering (SLS)

The radius of gyration and weight average molecular weight of the different pHPMAmDL-*b*-PEG micelles were determined by SLS at 37 °C at a concentration of 10 mg/mL in 120 mM ammonium acetate buffer (pH = 5.0). SLS experiments were carried out using multi-angle laser light scattering DAWN-DSP-F (MALLS, Wyatt Technology Corp., Santa Barbara, CA) equipped with a 5 mW He-Ne laser source (λ = 632.8 nm), a K5 glass flow cell, thermostated by a Peltier control of the temperature (36.7 ± 0.2 °C). The HPLC-system was equipped with a column (15 × 0.46 cm) packed with glass pearls (1.5 mm), placed in a column oven (Waters RCM-100/Column Heater), and was linked in series to the MALLS detector, a differential refractive index (RI) detector (ERMA ERC 7510) and a JASCO CD1595 UV detector. The MALLS instrument was calibrated to the scattering from HPLC-grade toluene, which has a high and accurately determined Rayleigh ratio, while the refractive index detector was calibrated using a saccharose solution in water. The injected

volume of micelle solution was 5 μL and the flow rate was 1.0 mL/min. During the chromatographic run, the MALLS detector measures simultaneously the degree of light scattering of the laser beam using detectors placed at 18 different angles ranging from 4.3° to 158.2°. For each sampling time of the elution pattern corresponding to one elution volume (V_i), the concentration (c_i) was calculated from the differential refractive index response. The data were analyzed for each individual slice "i" within the peak of interest using the algorithm from ASTRA software. Technically, the molar mass calculated for each slice from the fits, via Zimm, Debye, Berry or random coil plots, is weight averaged and the radius is z-averaged. These mass/radii can be used together with the concentration c_i, measured with the concentration sensitive detector, UV or RI, for each slice, to calculate the average mass for the entire peak. Following this determination, the intensity of the scattered light detected by the 15 Dawn-F photodiodes allows the determination of molecular weight (M_i) and radius of gyration ($R_i=\langle r_g^2\rangle_i^{1/2}$, where $\langle r_g^2\rangle_i$ is the mean square radius measured for the slice i) of the different micelles by ASTRA version 4.70.07 software, based on the equation:

$$\left(\frac{Kc}{R(\theta)}\right)_i = \frac{1}{M_i}\left(1+\frac{16\pi^2}{3\lambda^2}\left\langle r_g^2\right\rangle_i \sin^2(\theta/2)+2A_2M_ic_i\right)$$

where K is the optical constant defined as:

$$K=\frac{4\pi^2}{N_A\lambda^4}\frac{n_T^2}{R_T}\left(\frac{dn}{dc}\right)^2$$

n_T and R_T are the refractive index and Rayleigh ratio of toluene, respectively. N_A is Avogadro's constant, and (dn/dc) is the specific refractive index increment of the dispersion. R(θ) is the excess Rayleigh ratio of the solute (excess intensity of scattered light at DAWN angle θ), λ is the wavelength of the incident laser beam, and c_i is calculated from the differential refractive index response. A_2 is the second virial coefficient, M_i and R_i are obtained from the "y" intercept to zero scattering angle and from the slope, respectively. The weight average molecular weights of the micelles ($M_{w(mic)}$) is then calculated as

$$\overline{M_w}=\frac{\sum_i c_iM_i}{\sum_i c_i}$$

The root-mean-square z-average radius of gyration R_G^2 is

$$\overline{R}_G^2 = \left\langle \overline{r}_g^2 \right\rangle_z = \frac{\sum_i c_i M_i \left\langle r_g^2 \right\rangle_i}{\sum_i c_i M_i}$$

The density of the micelle was calculated by: $\rho_{mic} = M_{w(mic)}/N_a\ V$, where N_a is Avogadro's number and V is the average volume of the micelles. V was calculated based on the hydrodynamic radius (R_{hyd}) of micelles determined by DLS. The aggregation number of micelles (N_{agg}) was calculated by dividing $M_{w(mic)}$ by the number average molecular weight of block polymers determined by ^{1}H NMR (e.g. the M_n for pHPMAmDL(13600)-*b*-PEG(5000) is 18,600 g/mol). The surface area of the micelle's shell available per PEG chain (S/N_{agg}) was calculated by dividing S, the surface area of the shell of micelles calculated based on R_{hyd}, by N_{agg} [29].

2.8. Cryo-transmission electron microscopy (cryo-TEM)

Cryo-TEM measurements were performed on pHPMAmDL(13600)-*b*-PEG micelles prepared at a concentration of 10 mg/mL in 120 mM ammonium acetate buffer (pH = 5.0). Sample preparation for cryo-TEM was done in a temperature and humidity controlled chamber using a fully automated vitrification robot (FEI Company, Hillsboro, Oregon, USA) [30]. A thin aqueous film of micellar solution was formed on a Quantifoil R 2/2 grid (Quantifoil Micro Tools GmbH, Jena, Germany) at 22 °C and at 100 % relative humidity. The thin film was rapidly vitrified by shooting the grid into liquid ethane. The grids with the vitrified thin films were transferred into the microscope chamber using a Gatan 626 cryo-transfer/cryo-holder system (Gatan, Inc., Pleasanton, CA, USA). Micrographs were taken using a CM-12 transmission microscope (Philips, Eindhoven, The Netherlands) operating at 120 kV, with the specimen at –170 °C and using low-dose imaging conditions.

2.9. ^{1}H NMR measurements of block copolymers in D_2O

^{1}H NMR measurements were performed on pHPMAmDL(13600)-*b*-PEG block copolymer dissolved in D_2O (10 mg/mL) below the CMT (1 °C) and above the CMT (37 °C). The ^{1}H NMR spectra were recorded with an Inova 500 MHz spectrometer (Varian Associates Inc. NMR Instruments, Palo Alto, CA).

2.10. FT-IR measurements

FT-IR analysis was carried out with a Perkin-Elmer 2000 FT-IR instrument by accumulating 25 scans per spectrum at a data point resolution of 2 cm^{-1}. A spectrum of pHPMAmDL(13600)-*b*-PEG in KBr was recorded. Spectra of pHPMAmDL(13600)-*b*-PEG solutions (30 mg/mL in D_2O) were recorded by slowly heating a polymer solution in a 50 μm CaF_2 cell from below the CMT (2 °C) to above the CMT (50 °C) followed by cooling to 2 °C. Spectra were

recorded at different temperatures. A spectrum of D_2O recorded at 22°C was subtracted from all spectra.

2.11. Micelle destabilization

The destabilization of micelles was monitored at two different pH's (5.0 and 9.0). For pH 5.0, micelles of pHPMAmDL(13600)-*b*-PEG block copolymer were formed as described in Section 2.4 in isotonic 120 mM ammonium acetate buffer at a concentration of 2 mg/mL. For pH 9.0, the polymer was first dissolved in water at 20 mg/mL at 0 °C and then diluted 10-fold with 300 mM $NaHCO_3$ buffer (pH = 9.0). Micelles were formed as described in Section 2.4. Both the size of the micelles and the intensity of the scattered light were measured by DLS at 37 °C as a function of time. Pyrene-loaded micelles were prepared as described in Section 2.6. The pyrene concentration was 6.0×10^{-7} M and the concentration of pHPMAmDL(13600)-*b*-PEG block copolymer was 2 mg/mL. Then, 0.2 mL of pyrene-loaded micelle solution was added to 0.8 mL of isotonic 120 mM ammonium acetate buffer (pH = 5.0) or 300 mM $NaHCO_3$ buffer (pH = 9.0). The latter dilution gave a final pH of 8.6. Fluorescence measurements were performed as described in the Section 2.6 and the change of the ratio of I_{338}/I_{333} at 37 °C was monitored in time.

3. Results and Discussion

3.1. Synthesis and characterization of pHPMAmDL-b-PEG block copolymers

p(HPMAm-dilactate)-*b*-PEG block copolymers (pHPMAmDL-*b*-PEG) were synthesized by radical polymerization using HPMAm-dilactate as monomer and PEG_2-ABCPA as macroinitiator (Scheme 1). Table 1 summarizes the molecular characteristics of the synthesized copolymers. By changing the ratio of monomer to macroinitiator, three block copolymers with different pHPMAmDL block lengths (M_n from 3,000 to 13,600 g/mol, determined by ^1H NMR) and with a fixed PEG molecular weight (M_n = 5,000 g/mol) were obtained in yields between 75 and 80 %. In Chapter 2, it was shown that pHPMAmDL is a thermosensitive polymer with a cloud point (CP) around 10 °C in aqueous solution [24]. Consequently, it is expected that pHPMAmDL-*b*-PEG block copolymers can form micelles with hydrophilic PEG shells and hydrophobic pHPMAmDL cores above the CP of the pHPMAmDL blocks. The CMT of the block copolymers was determined by static light scattering. As shown in Table 1, the CMT decreased with increasing pHPMAmDL block lengths. A decreasing of CP with increasing molecular weight has also been observed for PNIPAAm [31] as well as for the homopolymer of HPMAmDL [24].

Table 1. Characteristics of pHPMAmDL-*b*-PEG block copolymers used in this study

Polymers	M_n [a]	M_w [a]	M_w/M_n	CMT (°C) [b]	CMC (mg/mL) [c]
pHPMAmDL(3000)-*b*-PEG [d]	7400	10400	1.41	12.5	0.15
pHPMAmDL(6900)-*b*-PEG [d]	11900	23300	1.95	7.5	0.03
pHPMAmDL(13600)-*b*-PEG [d]	15000	32800	2.18	6.0	0.015

[a] M_n = number average molar weight and M_w = weight average molar weight determined by GPC.
[b] Determined by SLS at a concentration of 10 mg/mL in 120 mM ammonium acetate buffer (pH = 5.0).
[c] Determined from pyrene excitation spectra for polymer solutions (Figure 2) in 120 mM ammonium acetate buffer (pH = 5.0) at 37 °C.
[d] Number in brackets is M_n of pHPMAmDL block determined by ^{1}H NMR. M_n of PEG is 5,000 g/mol.

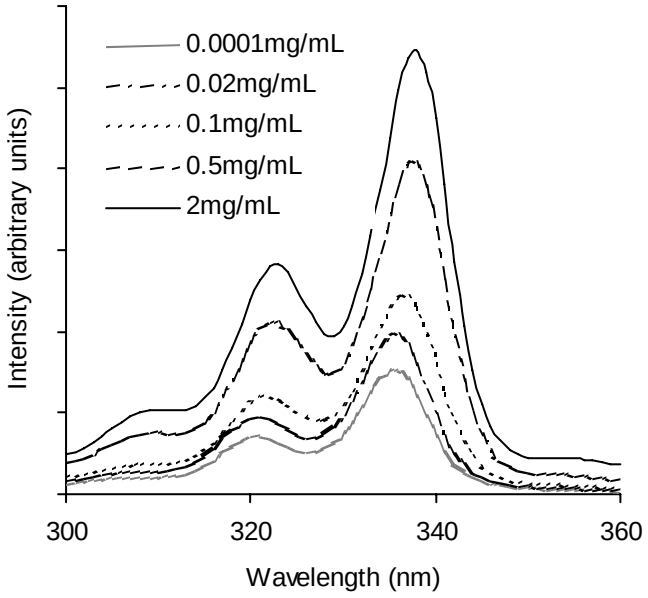

Figure 2. Fluorescence excitation spectra of pyrene (6.0×10^{-7} M) in 120 mM ammonium acetate buffer (pH = 5.0) containing pHPMAmDL(13600)-*b*-PEG at different concentrations. Emission wavelength = 390 nm.

The CMC of the block copolymers was determined using pyrene as a fluorescent probe. It is known that the fluorescent properties of pyrene largely depend on its microenvironment, and a red shift of the (0,0) band in its excitation spectra is observed when pyrene is partitioned from a hydrophilic to a more hydrophobic environment [28,32]. As shown in Figure 2, a red shift and intensity increase in the pyrene excitation spectra were observed with increasing

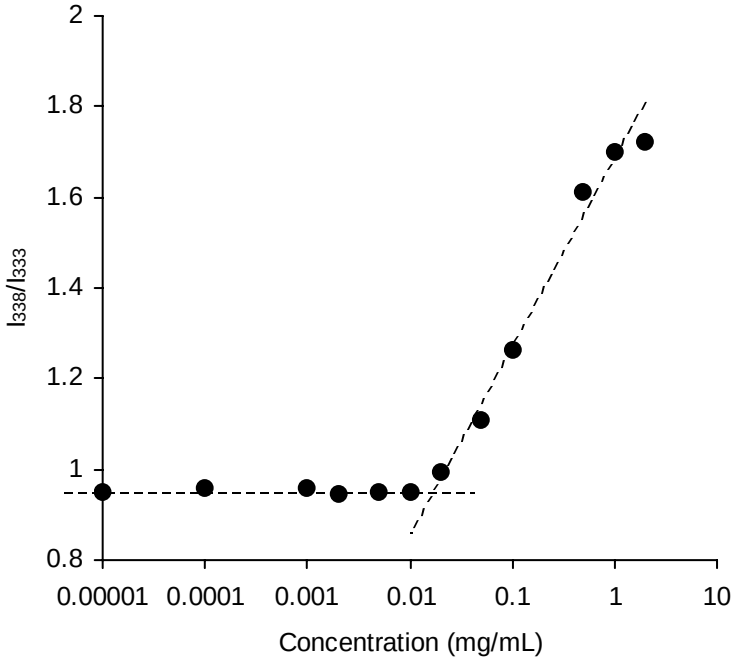

Figure 3. I_{338}/I_{333} ratio for pyrene as a function of the concentrations of pHPMAmDL(13600)-*b*-PEG. The CMC was taken from the intersection of the horizontal line at low polymer concentrations with the tangent of the curve at high polymer concentrations.

concentration of the pHPMAmDL-*b*-PEG block copolymer. The CMC could be accurately determined from the plot of the intensity ratio I_{338}/I_{333} as a function of the concentration of block copolymer (Figure 3). As expected, the CMC decreased with increasing pHPMAmDL block length (Table 1). The CMC values of pHPMAmDL(6900)-*b*-PEG and pHPMAmDL(13600)-*b*-PEG (0.03 and 0.015 mg/mL, respectively) are comparable to those of other amphiphilic block copolymers such as PBLA-*b*-PEG (0.005 to 0.018 mg/mL) [32,33] and PLA-*b*-PEG (0.0025 to 0.035 mg/mL) [34,35] which are appropriate for pharmaceutical applications. On the other hand, the CMC of pHPMAmDL(3000)-*b*-PEG is about 10-fold higher than those of the other two polymers, indicating an insufficient hydrophobicity of the pHPMAmDL(3000) block (containing ~10 monomer units of HPMAmDL) to form micelles at low concentration.

3.2.Characterization of micelles

It has been shown that the heating rate around the CMT is a critical parameter for the size of polymeric micelles based on thermosensitive polymers [27,36,37]. A rapid heating procedure favored the formation of small particles and was applied for the preparation of pHPMAmDL-*b*-PEG micelles. DLS

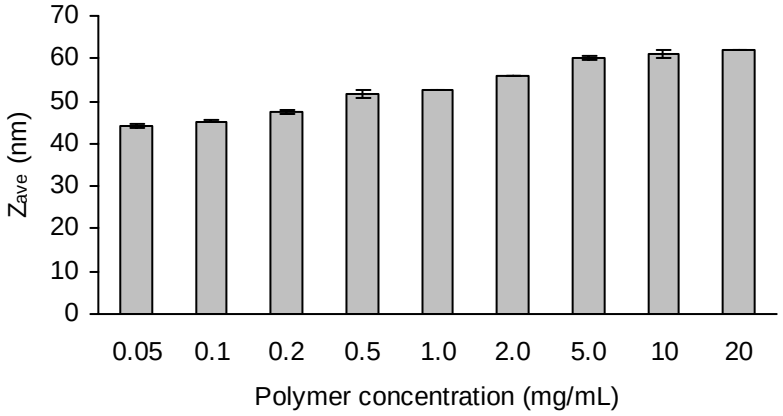

Figure 4. The effect of the polymer concentration on the size of pHPMAmDL(13600)-*b*-PEG micelles in isotonic 120 mM ammonium acetate buffer (pH = 5.0). The polydispersity index (PD) for the micelles was up to 10 mg/mL lower than 0.1; the PD for the micelles prepared at 20 mg/mL was 0.17. Data represent the mean and standard deviation of three independent experiments.

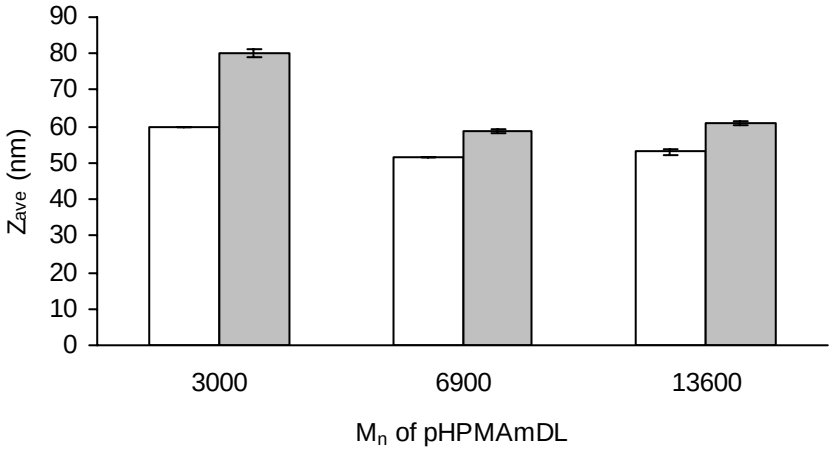

Figure 5. The effect of the pHPMAmDL block length on the size of pHPMAmDL-*b*-PEG micelles in isotonic 120 mM ammonium acetate buffer (pH = 5.0) at a concentration of 1 mg/mL (white bars) and 10 mg/mL (gray bars). Data represent the mean and standard deviation of three independent experiments.

measurements showed that micelles of pHPMAmDL(13600)-*b*-PEG with a size of 45 nm to 60 nm were obtained (Figure 4). During the formation of thermosensitive micelles upon heating, competition occurs between intrapolymer coil-to-globule transition (collapse) of the thermosensitive segments and interpolymer association. Smaller particles were formed with fast heating, owing to a rapid dehydration of the thermosensitive segments, and

therefore a collapse of these segments precedes the aggregation between polymers. As a result, micelles with well-defined core-shell structure are formed. In agreement with previous findings we found an increasing micelle size with increasing polymer concentration (Figure 4). This can be ascribed to higher probability of interpolymer aggregation at higher polymer concentration [27,36]. Figure 5 shows the effect of the pHPMAmDL block length on the size of micelles. pHPMAmDL(3000)-*b*-PEG formed, in particular at 10 mg/mL, larger micelles than the pHPMAmDL-*b*-PEG block copolymers with higher molecular weights of the thermosensitive segments. This observation is opposite to the results for PLA-*b*-PEG polymeric micelles, that showed a clear increase of their hydrodynamic diameter with increasing molecular weight of the PLA block [29]. As evidenced from static light scattering measurements (*vide infra*; Table 2), pHPMAmDL(3000)-*b*-PEG copolymers forms micelles with a rather low density likely due to relatively weak hydrophobic interactions of the low molecular weight pHPMAmDL, as also indicated by the high CMT and CMC values (Table 1).

The radius of gyration (R_g), and the weight average molecular weight ($M_{w(mic)}$) of the micelles composed of different block copolymers were determined by static light scattering (SLS) measurements at 37 °C (Table 2). The R_g/R_{hyd} ratio of pHPMAmDL-*b*-PEG micelles is between 0.59 and 0.80 and is in the same range as reported for other core-shell polymeric micelles [38-42]. Static light scattering measurements revealed that the aggregation number (N_{agg}) of pHPMAmDL(3000)-*b*-PEG micelles is 2-4 times lower than the N_{agg} of the other micelles. Despite this lower N_{agg}, DLS showed that pHPMAmDL(3000)-*b*-PEG micelles had the highest hydrodynamic radius (Figure 5 and Table 2). This indeed proves that the pHPMAmDL(3000) block is insufficiently hydrophobic to create a highly packed core structure and is reflected by a 10-20 fold lower ρ_{mic} value for the pHPMAmDL(3000)-*b*-PEG micelles than for the other systems. pHPMAmDL(6900/13600)-*b*-PEG micelles showed substantially higher ρ_{mic} and lower S/N_{agg} as compared to PLA-*b*-PEG with comparable molecular weights of both blocks and R_{hyd}. For example, PLA-*b*-PEG with M_n of PLA = 15,000 g/mol and M_n of PEG = 5,000 g/mol showed R_{hyd} = 25.3 nm, N_{agg} = 278, S/N_{agg} = 29 nm^2 and ρ_{mic} = 0.136 g/cm^3 [29]. This indicates that pHPMAmDL(6900/13600)-*b*-PEG forms micelles with a quite dense core. Furthermore, the very low value of S/N_{agg} (7-13 nm^2) for the pHPMAmDL(6900/13600)-*b*-PEG micelles demonstrates that their surfaces have a high PEG grafting density. This is a favorable property for drug delivery purposes, as it has been reported that colloidal particles showed increasing blood circulation times with increasing PEG surface grafting [35,43]. The low surface area for a PEG chain (S/N_{agg}) also indicates that PEG at the surface of pHPMAmDL(6900/13600)-*b*-PEG micelles exists in a highly stretched "brush" form.

Table 2. Characteristics of pHPMAmDL-*b*-PEG polymeric micelles at 10 mg/mL

Polymers	R_g [a] (nm)	R_{hyd} [b] (nm)	R_g/R_{hyd}	$M_{w(mic)}$ [a] ($\times 10^6$ Da)	ρ_{mic} [c] (g/cm^3)	N_{agg} [d]	S/N_{agg} [e] (nm^2)
pHPMAmDL(3000)-*b*-PEG	27 ± 1	40 ± 1	0.67 ± 0.04	3.3 ± 0.1	0.020	410	49.5
pHPMAmDL(6900)-*b*-PEG	17 ± 2	29 ± 1	0.59 ± 0.08	9.9 ± 0.2	0.16	830	12.7
pHPMAmDL(13600)-*b*-PEG	24 ± 2	30 ± 1	0.80 ± 0.08	32 ± 1	0.47	1720	6.6

[a] R_g = radius of gyration of micelles, $M_{w(mic)}$ = weight average molecular weight of micelles determined by SLS.
[b] R_{hyd} = hydrodynamic radius ($Z_{ave}/2$) of micelles determined by DLS.
[c] ρ_{mic} = density of the micelles.
[d] N_{agg} = aggregation number of the micelles.
[e] S/N_{agg} = surface area per PEG chain.
See Materials and methods for the calculation of ρ_{mic}, N_{agg} and S/N_{agg}.

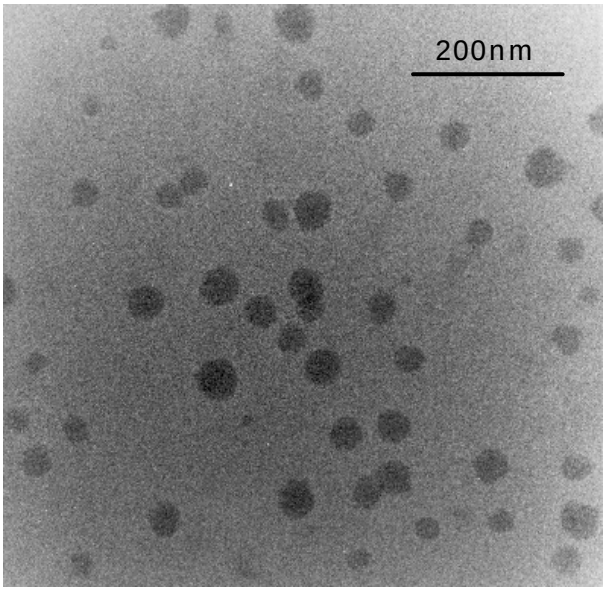

Figure 6. Cryo-TEM image of pHPMAmDL(13600)-*b*-PEG micelles. The polymer concentration was 10 mg/mL in 120 mM ammonium acetate buffer (pH = 5.0).

The morphology of pHPMAmDL(13600)-*b*-PEG micelles formed at 10 mg/mL was visualized by cryo-TEM. As shown in Figure 6, spherical structures with a narrow size distribution were observed. It should be noted that the outer PEG shells can not be seen with this technique because PEG is not electron-dense enough to be visualized without chemical staining. So, the observed spheres are the cores of the micelles that consist mainly of the pHPMAmDL block. The core size is between 25 nm and 50 nm and the average size is approximately 40 nm. The length of a PEG 5000 brush is 11.2 nm [44], suggesting that the average overall size of pHPMAmDL(13600)-*b*-PEG micelles is approximately 60 nm, which is in good agreement with the size as determined by DLS (Figure 4).

^{1}H NMR measurements were performed for pHPMAmDL(13600)-*b*-PEG in D_2O (10 mg/mL) below and above the CMT (Figure 7). This technique provides information on the mobility of polymer chains in aqueous solutions [29,45-47]. Below the CMT (1 °C), the intensity ratio of the peaks from pHPMAmDL block to the peak from PEG in D_2O was identical to that in $CDCl_3$, indicating that the pHPMAmDL chain is fully hydrated. On the other hand, above the CMT (37 °C), the peaks of the pHPMAmDL block almost completely disappeared while the intensity of signal of the PEG hydrogen atoms did not alter significantly (Figure 7). This indicates that the pHPMAmDL core of the micelles has a solid-like character. Around 20 % of the protons from the pHPMAmDL block can be still detected at 37 °C. Likely, pHPMAmDL segments adjacent to PEG and therefore located in the interfacial region of the core-shell structure of the micelles possess some flexibility and are therefore detectable with NMR [47].

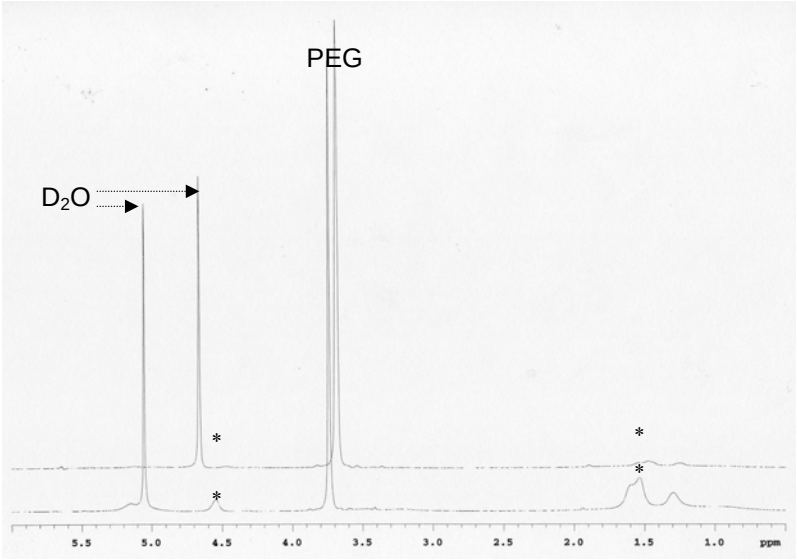

Figure 7. ^{1}H NMR spectra of pHPMAmDL(13600)-*b*-PEG in D_2O (10 mg/mL) at 1 °C (bottom) and at 37 °C (top). Asterisks represent peaks from pHPMAmDL blocks.

3.3. Mechanism of micelle formation

The mechanism of the micelle formation of pHPMAmDL(13600)-*b*-PEG block copolymer in aqueous solution was studied by FT-IR. Measurements were carried out for pHPMAmDL(13600)-*b*-PEG solutions at 30 mg/mL in D_2O at different temperatures below and above the CMT. The CMT of pHPMAmDL(13600)-*b*-PEG in D_2O at 30 mg/mL determined by SLS was 8.5 °C, while the CP in 120 mM ammonium acetate buffer was slightly lower (6.0 °C, Table 1), likely due to salting-out effects. Figure 8a shows the FT-IR spectra of the polymer in D_2O as a function of the temperature. As can be seen, some of the peaks are unaffected by changes in temperature, but the bands around 3400 cm^{-1} (N-H stretching vibration), 1735 cm^{-1} (C=O stretching), 1640 cm^{-1} (amide-I) and 1540 cm^{-1} (amide-II) shifted with temperature. Most striking are the changes of the amide-I and amide-II bands, showing from 2 to 50 °C a blue ($\Delta\nu$ = 5 cm^{-1}) and a red ($\Delta\nu$ = 12 cm^{-1}) shift, respectively (Figure 8b). A blue and red shift for the amide-I and amide-II vibrations has also been observed for PNIPAAm-*b*-PEG [21] and was explained by a change from hydrogen bonding of the amide groups with D_2O to intramolecular hydrogen bonding between amide groups above the CMT. The amide-I band exhibits the appearance of a shoulder at the low wavenumber side (1618 cm^{-1}; marked with an asterisk in Figure 8a) at low temperatures, which disappears at high temperatures. A possible explanation is that below the CMT, the amide group of pHPMAmDL has rotational freedom and may occur in both the *cis* and *trans* conformation, whereas above the CMT the mobility of the polymer chain is restricted by which the amide group is essentially in the more stable *trans* conformation.

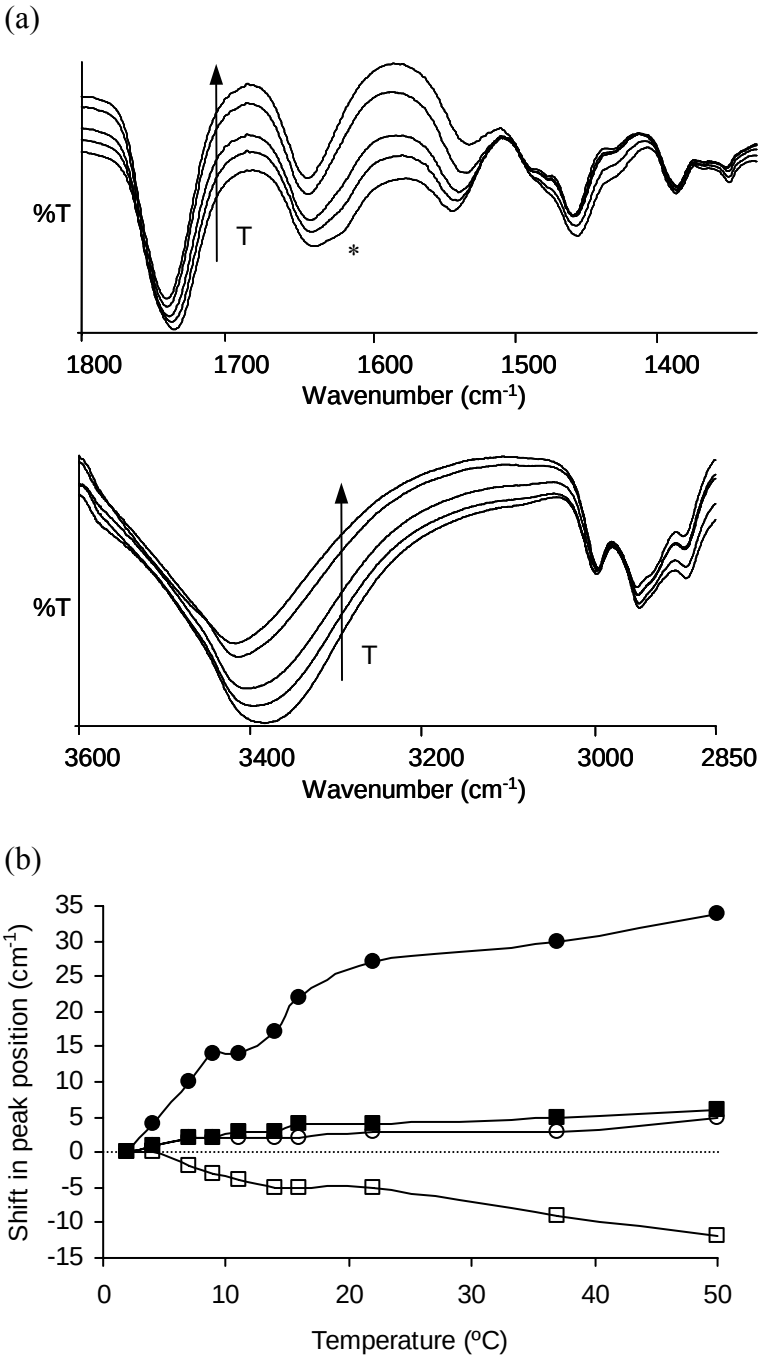

Figure 8. (a) FT-IR spectra of pHPMAmDL(13600)-*b*-PEG at 30 mg/mL in D_2O at different temperatures (50 °C, 37 °C, 16 °C, 9 °C and 2 °C from top to bottom, respectively). (b) The shift in peak position in FT-IR spectra as a function of temperature. The values are expressed as the difference of wavenumber compared to the peak position at 2 °C. Closed circles: N-H stretching (3382 cm^{-1} at 2 °C); Closed squares: C=O stretching (1734 cm^{-1} at 2 °C); Open circles: amide-I (1637 cm^{-1} at 2 °C); Open squares: amide-II (1541 cm^{-1} at 2 °C).

The observed peak position of the C=O stretching band of the lactic acid side groups (1734 to 1740 cm^{-1}) for pHPMAmDL(13600)-*b*-PEG in D_2O (above and below the CMT) is close to that for pHPMAmDL(13600)-*b*-PEG in the solid state (1744 cm^{-1}), but considerably higher than that of carbonyl groups that are subject to hydrogen bonding e.g. with D_2O (1710 to 1720 cm^{-1}) [48]. This indicates that even below the CMT the carbonyl groups of the lactic acid side groups in pHPMAmDL(13600)-*b*-PEG give no hydrogen bonding with D_2O. The peak around 3400 cm^{-1}, corresponding to the N-H stretching vibrations, is blue-shifted (34 cm^{-1}; Figure 8b) by heating. This again points to a dehydration of the amide bond with temperature. When the polymer dissolved in D_2O solution was heated from 2 to 50 °C and subsequently cooled to 2 °C, its IR spectrum was identical to that of the non-heated polymer solution. This demonstrates that the temperature induced phase transition of pHPMAmDL-*b*-PEG is completely reversible.

3.4. Destabilization of pHPMAmDL-b-PEG micelles

As suggested in Chapter 2 [24], one of the attractive features of pHPMAmDL is that its CP increases in time because of hydrolysis of the lactate side groups of pHPMAmDL in aqueous medium, as observed for the copolymer of HPMAmDL and NIPAAm [23]. As a result, pHPMAmDL is converted to the more hydrophilic poly(HPMAm-monolactate) (pHPMAmML), which has its CP around 65 °C [24], and finally to the water-soluble pHPMAm. Accordingly, polymeric micelles of pHPMAmDL-*b*-PEG are expected to gradually destabilize when incubated at physiological conditions (pH 7.4, 37 °C). At pH 5, where the hydrolysis of lactic acid side group is minimized [23], the micelles were very stable over 60 hours (Figure 9). On the other hand, at pH 9, where the hydrolysis is enhanced by hydroxyl ions [23], the size of the micelles and the scattering intensity started to increase after 1.5 hour of incubation, probably due to hydrophilization and subsequent swelling of the core. The micelles started to dissociate after 4 hours, as indicated by the disappearance of scattering, and finally a clear solution was obtained. Obviously the lactic acid side groups were hydrolyzed to such an extent that the CP of the thermosensitive block passed 37 °C. Previously it was shown that the hydrolysis of lactic acid side groups is a first order reaction in hydroxyl ion concentration [23], which means that 1 hour at pH 9.0 corresponds to 40 hours at pH 7.4 (physiological pH). Thus, at physiological condition, the swelling of micelles is supposed to start at 60 hours, and the dissolution of micelles occurs in 160 hours.

Pyrene-loaded pHPMAmDL(13600)-*b*-PEG micelles were incubated at 37 °C and at pH 5.0 and 8.6. As shown in Figure 10, the I_{338}/I_{333} ratio of pyrene loaded into the micelles was constant at pH 5.0 over 12 hours at 37 °C, indicating that the polarity of the microenvironment of pyrene (the hydrophobic core of the

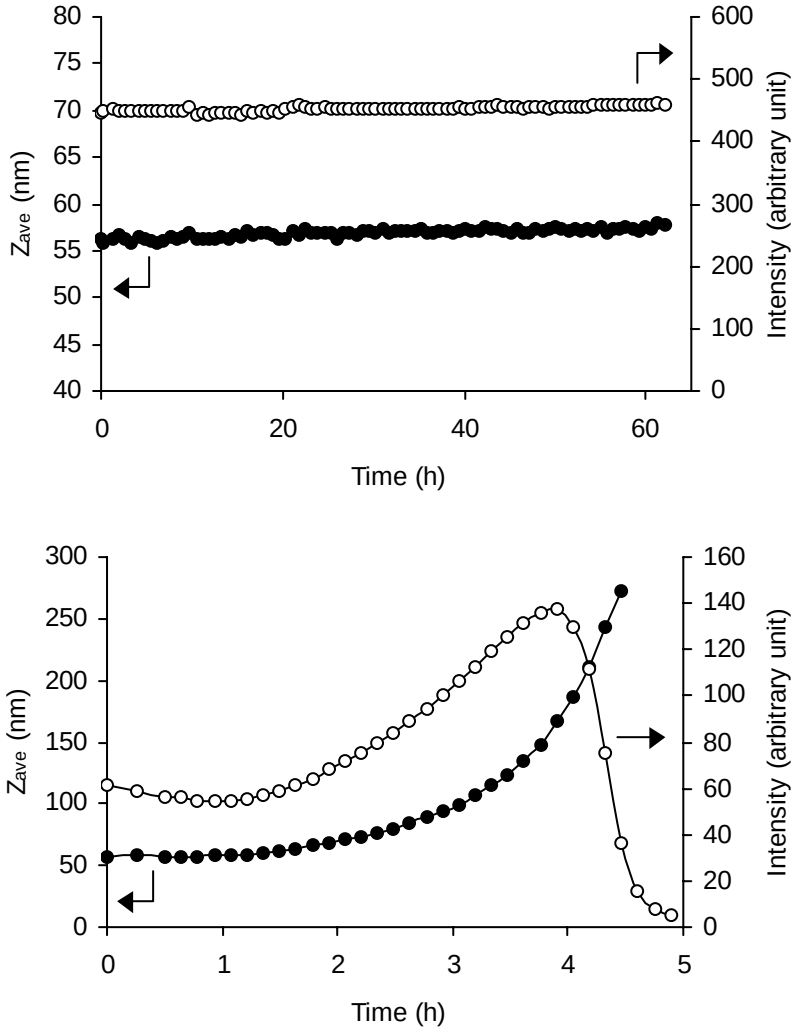

Figure 9. Stability of pHPMAmDL(13600)-*b*-PEG micelles at 37 °C and at pH 5.0 (top) and pH 9.0 (bottom), as determined by dynamic light scattering.

micelle) did not change in time. In contrast, the I_{338}/I_{333} ratio of pyrene in the micelles incubated at pH 8.6 decreased in time, indicating that the microenvironment of pyrene increased in polarity due to the ongoing hydrolysis of the lactic acid side groups and the resulting hydrophilization of the micellar core.

4. Conclusions

In this study, novel thermosensitive and biodegradable block copolymers, pHPMAmDL-*b*-PEG, were synthesized. Stable polymeric micelles with a size around 50 nm were obtained when aqueous solutions of pHPMAmDL(6900/13600)-*b*-PEG were heated above the CMT. ^{1}H NMR and static light scattering measurements demonstrate that the micelles have solid-

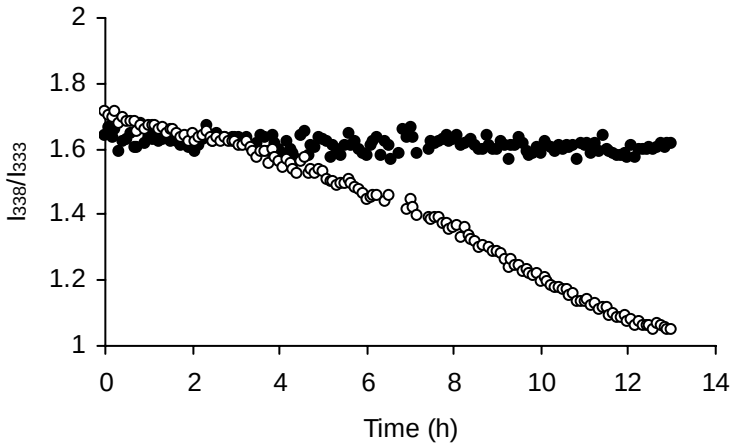

Figure 10. Change in emission spectra (I_{338}/I_{333} ratio) of pyrene solubilized in pHPMAmDL(13600)-*b*-PEG micelles at 37 °C and at pH 5.0 (closed circles) and pH 8.6 (open circles).

like and dense core structures and that the hydrophobic core is stabilized with a hydrophilic PEG corona. Importantly, it was found that pHPMAmDL-*b*-PEG micelles showed a controlled instability due to hydrolysis of the lactic acid side chains in the thermosensitive block. Furthermore, the dense and stable core of the micelles should allow the loading of hydrophobic drugs. These features, together with the simple preparation method, avoiding the use of organic solvents, make these micelles very suitable as delivery vehicles for hydrophobic drugs.

Acknowledgements

The authors thank Mitsubishi Pharma Corporation (Japan) for their financial support. The authors thank Dr Johan Kemmink for his assistance with the ^{1}H NMR measurements and Professor Kees de Kruif, Mr. Kees Olie man and Mr. Jan Klok from Nizo food research, Ede, The Netherlands, for their help in performing the light scattering measurements.

References

1. S. Forster, T. Plantenberg. *Angew Chem Int Ed Engl* 41 (2002) 689-714.
2. G. Riess. *Prog Polym Sci* 28 (2003) 1107-1170.
3. C. Allen, D. Maysinger, A. Eisenberg. *Colloids Surf B: Biointerfaces* 16 (1999) 3-27.
4. M.C. Jones, J.C. Leroux. *Eur J Pharm Biopharm* 48 (1999) 101-111.
5. K. Kataoka, A. Harada, Y. Nagasaki. *Adv Drug Deliv Rev* 47 (2001) 113-131.

6. G.S. Kwon. *Crit Rev Ther Drug Carrier Syst* 20 (2003) 357-403.
7. G.S. Kwon, M. Naito, M. Yokoyama, T. Okano, Y. Sakurai, K. Kataoka. *Pharm Res* 12 (1995) 192-195.
8. H. Maeda, J. Wu, T. Sawa, Y. Matsumura, K. Hori. *J Control Release* 65 (2000) 271-284.
9. G. Molineux. *Cancer Treat Rev* 28 (2002) 13-16.
10. M.C. Woodle, D.D. Lasic. *Biochim Biophys Acta* 1113 (1992) 171-199.
11. A.V. Kabanov, E.V. Batrakova, V.Y. Alakhov. *J Control Release* 82 (2002) 189-212.
12. M. Yokoyama, S. Fukushima, R. Uehara, K. Okamoto, K. Kataoka, Y. Sakurai, T. Okano. *J Control Release* 50 (1998) 79-92.
13. R.T. Liggins, H.M. Burt. *Adv Drug Deliv Rev* 54 (2002) 191-202.
14. R. Savic, L. Luo, A. Eisenberg, D. Maysinger. *Science* 300 (2003) 615-618.
15. Y.H. Bae, S. Fukushima, A. Harada, K. Kataoka. *Angew Chem Int Ed Engl* 42 (2003) 4640-4643.
16. J. Taillefer, M.C. Jones, N. Brasseur, J.E. van Lier, J.C. Leroux. *J Pharm Sci* 89 (2000) 52-62.
17. H.G. Schild. *Progress in Polymer Science* 17 (1992) 163-249.
18. R. Pelton. *Adv Colloid Interface Sci* 85 (2000) 1-33.
19. S. Fujishige, K. Kubota, I. Ando. *J Phys Chem* 93 (1989) 3311-3313.
20. M.D.C. Topp, P.J. Dijkstra, H. Talsma, J. Feijen. *Macromolecules* 30 (1997) 8518-8520.
21. Y. Maeda, N. Taniguchi, I. Ikeda. *Macromol Rapid Commun* 22 (2001) 1390-1393.
22. D. Neradovic, C.F. van Nostrum, W.E. Hennink. *Macromolecules* 34 (2001) 7589-7591.
23. D. Neradovic, M.J. van Steenbergen, L. Vansteelant, Y.J. Meijer, C.F. van Nostrum, W.E. Hennink. *Macromolecules* 36 (2003) 7491-7498.
24. O. Soga, C.F. van Nostrum, W.E. Hennink. *Biomacromolecules* 5 (2004) 818-821.
25. J. Kopecek, P. Kopeckova, T. Minko, Z. Lu. *Eur J Pharm Biopharm* 50 (2000) 61-81.
26. R. Duncan. *Nat Rev Drug Discov* 2 (2003) 347-360.
27. D. Neradovic, O. Soga, C.F. van Nostrum, W.E. Hennink. *Biomaterials* 25 (2004) 2409-2418.
28. M. Wilhelm, C.L. Zhao, Y.C. Wang, R.L. Xu, M.A. Winnik, J.L. Mura, G. Riess, M.D. Croucher. *Macromolecules* 24 (1991) 1033-1040.
29. T. Riley, S. Stolnik, C.R. Heald, C.D. Xiong, M.C. Garnett, L. Illum, S.S. Davis, S.C. Purkiss, R.J. Barlow, P.R. Gellert. *Langmuir* 17 (2001) 3168-3174.
30. A. Moschetta, P.M. Frederik, P. Portincasa, G.P. vanBerge-Henegouwen, K.J. van Erpecum. *J Lipid Res* 43 (2002) 1046-1053.
31. E.I. Tiktopulo, V.N. Uversky, V.B. Lushchik, S.I. Klenin, V.E. Bychkova, O.B. Ptitsyn. *Macromolecules* 28 (1995) 7519-7524.
32. G. Kwon, M. Naito, M. Yokoyama, T. Okano, Y. Sakurai, K. Kataoka. *Langmuir* 9 (1993) 945-949.

33. S.B. La, T. Okano, K. Kataoka. *J Pharm Sci* 85 (1996) 85-90.
34. K. Yasugi, Y. Nagasaki, M. Kato, K. Kataoka. *J Control Release* 62 (1999) 89-100.
35. S.A. Hagan, A.G.A. Coombes, M.C. Garnett, S.E. Dunn, M.C. Davis, L. Illum, S.S. Davis, S.E. Harding, S. Purkiss, P.R. Gellert. *Langmuir* 12 (1996) 2153-2161.
36. P.W. Zhu, D.H. Napper. *Langmuir* 16 (2000) 8543-8545.
37. X.P. Qiu, C. Wu. *Macromolecules* 30 (1997) 7921-7926.
38. M.R. Talingting, P. Munk, S.E. Webber, Z. Tuzar. *Macromolecules* 32 (1999) 1593-1601.
39. H. Schuch, J. Klingler, P. Rossmanith, T. Frechen, M. Gerst, J. Feldthusen, A.H. Muller. *Macromolecules* 33 (2000) 1734-1740.
40. S. Dai, P. Ravi, C.Y. Leong, K.C. Tam, L.H. Gan. *Langmuir* 20 (2004) 1597-1604.
41. P. Ravi, C. Wang, K.C. Tam, L.H. Gan. *Macromolecules* 36 (2003) 173-179.
42. S. Pispas, N. Hadjichristidis, I. Potemkin, A. Khokhlov. *Macromolecules* 33 (2000) 1741-1746.
43. S. Stolnik, B. Daudali, A. Arien, J. Whetstone, C.R. Heald, M.C. Garnett, S.S. Davis, L. Illum. *Biochim Biophys Acta* 1514 (2001) 261-279.
44. D. Marsh, R. Bartucci, L. Sportelli. *Biochim Biophys Acta* 1615 (2003) 33-59.
45. J.S. Hrkach, M.T. Peracchia, A. Domb, N. Lotan, R. Langer. *Biomaterials* 18 (1997) 27-30.
46. Y. Yamamoto, K. Yasugi, A. Harada, Y. Nagasaki, K. Kataoka. *J Control Release* 82 (2002) 359-371.
47. C.R. Heald, S. Stolnik, K.S. Kujawinski, C. De Matteis, M.C. Garnett, L. Illum, S.S. Davis, S.C. Purkiss, R.J. Barlow, P.R. Gellert. *Langmuir* 18 (2002) 3669-3675.
48. L.J. Bellamy. *Advances in Infrared Group Frequencies*, Methuen, London (1968).